Antagonizing the hedgehog pathway with vismodegib impairs malignant pleural mesothelioma growth in vivo by affecting stroma

Meerang, Mayura ; Bérard, Karima ; Felley-Bosco, Emanuela ; Lauk, Olivia ; Vrugt, Bart ; Boss, Andreas ; Kenkel, David ; Broggini-Tenzer, Angela ; Stahel, Rolf A ; Arni, Stephan ; Weder, Walter ; Opitz, Isabelle

Abstract: An autocrine driven upregulation of the Hedgehog (Hh) signaling pathway has been described in malignant pleural mesothelioma (MPM), in which the ligand, desert hedgehog (DHH), was produced from tumor cells. However, our investigation revealed that the Hh pathway is activated in both tumor and stroma of MPM tumor specimens and an orthotopic immunocompetent rat MPM model. This was demonstrated by positive immunohistochemical staining of Glioma associated oncogene 1 (GLI1) and Patched1 (PTCH1) in both tumor and stromal fractions. DHH was predominantly expressed in the tumor fractions. To further investigate the role of the Hh pathway in MPM stroma, we antagonized Hh signaling in the rat model of MPM using a Hh antagonist, vismodegib, (100 mg/kg peroral). Daily treatment with vismodegib efficiently downregulated Hh target genes, Gli1, Hedgehog Interacting Protein (Hhip) and Ptch1, and caused a significant reduction of tumor volume, and tumor growth delay. Immunohistochemical analyses revealed that vismodegib treatment primarily down regulated GLI1 and HHIP in the stromal compartment along with a reduced expression of previously described fibroblast Hh responsive genes such as Fibronectin (Fn1) and Vegf. Primary cells isolated from the rat model cultured in 3%O2 continued to express Dhh but did not respond to vismodegib in vitro. However, culture supernatant from these cells stimulated Gli1, Ptch1, and Fn1 expression in mouse embryonic fibroblasts which was suppressed by vismodegib. Our study provides new evidence regarding the role of Hh signaling in MPM stroma in the maintenance of tumor growth, emphasizing Hh signaling as a treatment target for MPM.

DOI: https://doi.org/10.1158/1535-7163.MCT-15-0583

Author Manuscript Published OnlineFirst on February 2, 2016; DOI: 10.1158/1535-7163.MCT-15-0583
Author manuscripts have been peer reviewed and accepted for publication but have not yet been edited.

Title page

Antagonizing the Hedgehog Pathway with Vismodegib Impairs Malignant Pleural Mesothelioma Growth *In Vivo* by Affecting Stroma

Authors and affiliations:

Mayura Meerang[1], *Karima Bérard*[1], *Emanuela Felley-Bosco*[2], *Olivia Lauk*[1], *Bart Vrugt*[3], *Andreas Boss*[4], *David Kenkel*[4], *Angela Broggini-Tenzer*[5], *Rolf A. Stahel*[6], *Stephan Arni*[1], *Walter Weder*[1], *Isabelle Opitz*[1]

[1] Division of Thoracic Surgery, University Hospital Zurich

[2] Laboratory of Molecular Oncology, University Hospital Zurich

[3] Institute of Surgical Pathology, University Hospital Zurich

[4] Institute of Diagnostic and Interventional Radiology, University Hospital Zurich

[5] Laboratory for Molecular Radiobiology, Radiation Oncology, University Hospital Zurich

[6] Clinic for Oncology, University Hospital Zurich

Running title: (60 characters)

Vismodegib reduces mesothelioma growth by affecting stroma

Keywords: (5)

Malignant Pleural Mesothelioma, Vismodegib, Hedgehog, Immunocompetent orthotopic rat model, stroma

Financial support: The project is financed by the Swiss National Science Foundation to I. Opitz (grant number: PP00P3_159269).

No conflict of interest

Corresponding author:

Isabelle Opitz

Division of Thoracic Surgery

University Hospital Zurich

Rämistrasse 100

CH 8091 Zürich, Switzerland

Tel: +41-44-255-9299

FAX: +41-44-255-8805

E-mail: isabelle.schmitt-opitz@usz.ch

Abstract

An autocrine driven upregulation of the Hedgehog (Hh) signaling pathway has been described in malignant pleural mesothelioma (MPM), in which the ligand, desert hedgehog (DHH), was produced from tumor cells. However, our investigation revealed that the Hh pathway is activated in both tumor and stroma of MPM tumor specimens and an orthotopic immunocompetent rat MPM model. This was demonstrated by positive immunohistochemical staining of Glioma associated oncogene 1 (GLI1) and Patched1 (PTCH1) in both tumor and stromal fractions. DHH was predominantly expressed in the tumor fractions. To further investigate the role of the Hh pathway in MPM stroma, we antagonized Hh signaling in the rat model of MPM using a Hh antagonist, vismodegib, (100 mg/kg peroral). Daily treatment with vismodegib efficiently downregulated Hh target genes, *Gli1, Hedgehog Interacting Protein (Hhip) and Ptch1,* and caused a significant reduction of tumor volume, and tumor growth delay. Immunohistochemical analyses revealed that vismodegib treatment primarily down regulated GLI1 and HHIP in the stromal compartment along with a reduced expression of previously described fibroblast Hh responsive genes such as *Fibronectin* (*Fn1)* and *Vegf*. Primary cells isolated from the rat model cultured in 3%O_2 continued to express *Dhh* but did not respond to vismodegib *in vitro*. However, culture supernatant from these cells stimulated *Gli1*, *Ptch1,* and *Fn1* expression in mouse embryonic fibroblasts which was suppressed by vismodegib. Our study provides new evidence regarding the role of Hh signaling in MPM stroma in the maintenance of tumor growth, emphasizing Hh signaling as a treatment target for MPM.

Introduction

Malignant Pleural Mesothelioma (MPM), an aggressive cancer most often caused by asbestos exposure, is still a public health concern. MPM arises from malignant transformation of the mesothelial cell layer lining the pleural cavity (1). About 80% of MPM cases are related to asbestos exposure, further causes are other environmental exposures and genetic predisposition. Incidence rates in Western European nations and Australia are still rising with expected peak around 2020 and beyond (2) due to long disease latency (3). The prognosis of MPM remains poor. Intensive multimodal regimen combining chemotherapy, surgery and radiotherapy contributed to a median overall survival of 24 months (4). Currently, other treatment options including molecular targeted therapy as well as immunotherapy are being a focus of interest.

Recent findings of the activated Hedgehog (Hh) signaling pathway in MPM have underlined its role as a target for MPM treatment (5-7). The Hh pathway is one of the crucial stem cell signaling pathways that regulate embryonic development and adult tissue repair (8). In the absence of Hh ligand binding, the receptor Patched (PTCH1) represses the transmembrane G protein-coupled receptor Smoothened (SMO). Binding of ligands (Sonic hedgehog (SHH), Indian hedgehog (IHH) and Desert hedgehog (DHH)) to PTCH1 unleashes SMO to induce Hh pathway activation *via* an intracellular signaling cascade. The transcription factors glioma-associated oncogenes 1-3 (GLI1, GLI2 and GLI3) convey the cytoplasmic signal and induce transcription of pro-proliferative and anti-apoptotic target genes, such as *GLI1*, *PTCH1*, *Hedgehog interacting protein* (*HHIP*), *CyclinD1* or *BCL2* (8) depending on cell type and situation. Constitutive pathway activation resulting from mutations of pathway components is frequently detected in sporadic basal cell carcinoma (BCC) and medulloblastoma (MB) (9, 10). Furthermore, aberrant up-regulation of Hh pathway in ligand dependent (paracrine or autocrine) manner has been described in hematologic malignancies and several solid tumors (11). Studies in colon and pancreatic adenocarcinoma demonstrated the paracrine activation of Hh signaling (12, 13). In these studies, human tumor cells cultured *in vitro* did not respond to a SMO antagonist. In contrast, the treatment with the SMO antagonist in subcutaneous tumor xenograft resulted in delayed tumor growth. Gene expression analyses suggested that only murine stroma but not tumor epithelium could respond to SMO antagonist explaining the lack of response *in vitro* (12, 13). Co-culture experiments further showed the paracrine activation of Hh signaling in lung and

prostate cancer (14, 15). These highlight the importance of Hh signaling in tumor and thus serves as a rational for a treatment targeting cancer (11).

In MPM, increased *SHH* and *GLI1* mRNA expression was detected in tumor tissues compared to normal mesothelium (5). High *GLI1* expression (5) and high SMO and SHH protein levels (6) were associated with poor survival of MPM patients. Recent data from The Cancer Genome Atlas (TCGA) demonstrated that the Hh pathway is among the top 10 most deregulated pathways in MPM [Reviewed in (16)]. Altogether, these data underline the importance of the Hh pathway in MPM. Nevertheless, mutations of Hh pathway components in MPM were reported to be relatively rare (17). So far, up-regulation of the Hh signaling in MPM has been demonstrated in ligand dependent autocrine manner, interestingly only mediated by DHH in the primary culture in 3% O_2 without serum (5). It is important to note that 2 out of 6 MPM primary cells employed in that study were not responsive to a SMO antagonist (5) suggesting a possible role of paracrine activation in MPM. Indeed, here we provide new evidence regarding paracrine Hh activation in MPM. Using an immunocompetent orthotopic rat MPM model, we demonstrated that Hh pathway activation in stroma plays a role in the maintenance of tumor growth.

Materials and Methods

Patient tissue samples

Eight diagnostic MPM tumor specimens and two tissue micro arrays from 138 patients collected between 1999-2009 were employed. The study was approved by the institutional review board (ethical approval numbers: StV 29-2009 and EK-ZH 2012-0094) and all patients received and signed a written inform consent. Formalin-fixed paraffin-embedded tissues were cut into 3 µm thick slices and processed for immunohistochemistry and scored semi-quantitatively as described below.

Cell culture

Rat mesothelioma cell line IL45 was originally produced in rat exposed intraperitoneally to asbestos (18). IL45 expressing luciferase (IL45-*luc*) was generated by us in 2011 by stable transfection of IL45 with luciferase expressing vector (19). Both IL45 and IL45-*luc* were maintained in RPMI1640 containing 1mM sodium pyruvate, Penicillin/Streptomycin (P/S), 200 µg/ml Geneticin (G418) and 10% fetal bovine serum (FBS) at 37°C with 5% CO_2. NIH3T3, employed for Hh activity assay as described in the previous publication (5), were maintained in RPMI (ATCC modification) supplemented with 10% FBS and 1% P/S at 37° C, 5% CO_2. Rat and mouse cell lines employed in

Author Manuscript Published OnlineFirst on February 2, 2016; DOI: 10.1158/1535-7163.MCT-15-0583
Author manuscripts have been peer reviewed and accepted for publication but have not yet been edited.

this study were tested for the absence of *Mycoplasma* but were not authenticated by us. Primary culture of tumors was performed using the previously described method ((6); and maintained in medium w/o serum (Dulbecco's Modified Eagle's Media:F12, 0.4 µg/mL hydrocortisone, 10 ng/mL rat-EGF, 20 ng/mL rat-basic fibroblast growth factor, 10 µg/mL insulin, 5.5 µg/mL transferrin, 6.7 µg/mL selenium, 1 mmol/L sodium pyruvate, 100 µmol/L β-mercaptoethanol, nonessential amino acids and 30% own conditioned medium) at 37°C, 5%O_2, 3%O_2.

***In vitro* treatment with vismodegib, viability and colony formation assay**

Vismodegib was prepared in DMSO and stored at -20°C. Working dilutions were freshly prepared in culture medium containing 0.5% FBS. A viability assay of the IL45-*luc* monolayer cells was performed using Methylthiazolyldiphenyl-tetrazolium bromide (MTT) after 72 hour treatment. Primary IL45-*luc* derived from tumors maintained in 3% O_2 without serum formed clumps and spheres. For this reason, the acid phosphatase (APH) assay using ImmunoPure p-nitrophenyl phosphate substrate (20) was employed to measure their viability. Colony formation assay was performed in 0.5% FBS. Cells were treated with vismodegib for 10 days, and stained with crystal violet and analyzed under a light microscope where colonies with ≥ 5 cells were counted. All results were confirmed in at least 3 independent experiments.

NIH3T3 treatment with cell culture supernatant

Supernatant from primary culture of rat tumors were harvested freshly, after centrifugation at 400 g for 5 minutes. Supernatant from a primary human MPM culture was harvested and kept at 4ºC until used. NIH3T3 cells were seeded in a 6 well plate at 900,000 cells/well in the complete medium. After overnight incubation at atmospheric oxygen level, the medium were then replaced by supernatant from primary culture mixed with 0.05% DMSO or vismodegib. SMO agonist (SAG: Abcam; Ab142160) was employed as a positive control. SAG powder was dissolved in DMSO and stored at -20ºC. Working dilution of SAG was freshly prepared and added to culture medium used for rat primary culture. After receiving the treatment, NIH3T3 were incubated at 37°C, 5%CO_2 and 3%O_2. Cells were harvested at 72 hour later for RNA extraction. The results were confirmed by at least 2 independent experiments except for the treatment with human MPM supernatant where no material was available for the duplication.

Orthotopic rat MPM model and treatment

The experimental scheme is depicted in figure 3a. The animal experiment was authorized by the veterinary office of canton Zurich, Switzerland (112/2013). Male Fischer 344 rats (n=12, 200-250

Author Manuscript Published OnlineFirst on February 2, 2016; DOI: 10.1158/1535-7163.MCT-15-0583
Author manuscripts have been peer reviewed and accepted for publication but have not yet been edited.

grams; Harlan Laboratories, the Netherland) were housed according to the guideline for animal welfare. A sterile 50 µl of 500,000 IL45-*luc* cell suspension in Dulbecco's Phosphate Buffered Saline (DPBS) was implanted underneath the parietal pleura using a surgical procedure as previously described (21). In order to start with the same tumor size, the treatment started when the tumor was first detectable by bioluminescence (Bli) (between 2-6 days after implantation). Vismodegib free base (LC laboratories, V-4050) was dissolved in 0.5% Methylcellulose/0.2% Tween (MCT) solution and sonicated. The drug suspension was freshly prepared and administered once daily for 6 days by oral gavage at a dosage of 100 mg/kg (22). Control animals received only MCT. Once the treatment started, Bli was performed every second day until day 6. Magnetic resonance imaging (MRI) was performed after Bli measurement at day 6 prior to euthanasia. Macroscopic tumor volume was measured at autopsy using the ellipsoid volume formula V= 4/3 π * a/2 * b/2 * c/2 (a=length, b=width, c=thickness measured on H&E sections).

Tumor imaging

MRI was performed using a 4.7 Tesla small animal MR scanner equipped with a ^{1}H whole-body rat coil (Bruker 4.7-T PharmaScan 47/16 US). MR data sets were acquired applying T2-weighted fast spin-echo sequences in transverse/sagittal/coronal orientation (repetition time TR 3500 ms, echo time TE 45 ms). The tumor volume (mm^3) was quantified blindly with Image J software (NIH, MD) by 2 observers as we described previously (23).

Bli was performed in the imaging chamber of the IVIS200 (Caliper Life Sciences, Inc., MA, USA)**.** Prior to the imaging procedure, rats were injected with 150 mg/kg body weight Xenolight D-Luciferin –K+ salt (Perkin Elmer, 122796; dissolved in sterile DPBS). Bli measurement was recorded over 30 minutes with the exposure time of 60 seconds. When the maximum Bli signal was reached (in about 15-25 minutes), region of tumor was measured for Bli signal intensity (total flux; photon/second).

RNA extraction and quantitative real time PCR

RNA extraction was performed using Trizol® reagent (Ambion®, 15596-018) according to manufacturer´s instructions. 500 ng of total RNA was used for cDNA synthesis using RT^2 first strand kit (Qiagen, 205311). Quantitative real time PCR was performed using *Power* SYBR® green PCR mastermix (Applied biosystems®, 4368577). Primers are listed in the supplementary table 1 or were previously described (24, 25). The reaction was performed in triplicate and normalized with a loading control, *Histone H3* for rat cells and *Beta actin* (*Acbt*) for mouse cells (26). Relative quantitation (RQ)

Author Manuscript Published OnlineFirst on February 2, 2016; DOI: 10.1158/1535-7163.MCT-15-0583
Author manuscripts have been peer reviewed and accepted for publication but have not yet been edited.

of gene expression was calculated using the $2^{-\Delta\Delta Ct}$ method. For *in vivo* samples, the following relative quantitation was applied $RQ=2^{-(C_{t,target}-C_{t,H3})/(\text{average } C_{t,target}-C_{t,H3} \text{ of control group})}$.

Tissue processing and immunohistochemistry

Tumor tissues were collected and immediately fixed in formalin. They were de-calcified in neutral EDTA pH 7.0 for 2-4 weeks before paraffin embedding. Tissues were cut into 3 µm slices and rehydrated through series of graded alcohol followed by immunohistochemistry using the following antibodies: GLI1 (Santa Cruz, H-300), Fibronectin (Abcam, ab6328), DHH (Santa Cruz, H-19), PTCH1 (Aviva Systems Biology, ARP44249_P050), HHIP (Santa Cruz , H-280), Ki-67 (Cell Marque, CMC27531021), phospho-histone H3 (ser10) (Cell Signaling, #9701).

GLI1 and DHH antigen retrieval was achieved by 20 minutes microwave (700 watt) cooking in sodium citrate buffer pH 6.0. After overnight incubation with primary antibodies at 4°C, the secondary antibody was applied followed by Vectastain ABC Reagent (Vector laboratories). DAB chromogen (Dako) was applied for visualization of the signals and counterstained with haematoxylin. PTCH1 and HHIP were stained with Dako Autostainer Link48 Instrument (Dako Denmark A/S). Antigen retrieval for PTCH1 was performed using target retrieval solution high pH (Dako, K8004, 20 min, 97°C). For HHIP, target retrieval solution low pH (Dako, K8005; 20 min, 97°C) was employed for rat tissues and target retrieval solution high pH (Dako, K8004; 20 min, 97°C) was employed for human tissues. The visualization system consisted of the Dako EnVision™ Rabbit/HRP/DAB system and haematoxylin as counterstain. TUNEL staining was conducted on the Leica-bond RX automater using digoxigenein labelled dUTP (Roche, 11570013910) and terminal deoxynucleotidyl transferase (Promega, M1875) after enzymatic retrieval (Sophistolab AG, Muttenz, Switzerland).

Quantitation of immunohistochemistry

Images were captured with a light microscope (Leica DM6000). H-scoring system was applied to semi-quantitatively quantify protein expression by 3 observers (K.B, M.M and B.V.). Staining intensity was scored 0-3 (negative-strong). Staining frequency was set as 0.1 (<10% positive cells), 0.5 (10-50% positive cells), 1 (>50% positive cells). The H-score was the multiplication of intensity and frequency (range 0-3). Proliferation, mitotic and TUNEL positive indices were calculated by counting positive tumor nuclei per total tumor cells (at least 1000 total cells).

Statistical analysis

The differences between means were verified by unpaired two-sided t-tests using the GraphPad Prism software. A statistical significant difference was defined for P values ≤ 0.05.

Author Manuscript Published OnlineFirst on February 2, 2016; DOI: 10.1158/1535-7163.MCT-15-0583
Author manuscripts have been peer reviewed and accepted for publication but have not yet been edited.

Results

Hh pathway is activated in tumor and in stroma of human MPM

Eight MPM tumor specimens including 6 epithelioid, 1 biphasic and 1 sarcomatoid were analyzed for the expression of GLI1, DHH, PTCH1 and HHIP by immunohistochemistry (figure 1a). In addition two TMAs consisting of 138 patients (89 epithelioid, 41 biphasic and 8 sarcomatoid) were analyzed for GLI1 and DHH expression. GLI1 is expressed in both tumor and stromal fractions in all the samples assessed. When comparing tumor and stroma, DHH, PTCH1 and HHIP expression is higher in the tumor fraction (figure 1a).

Hh pathway is activated in tumor and in stroma of an orthotopic immunocompetent rat model of mesothelioma

To investigate the role of Hh signaling in MPM stroma, we employed our previously described rat MPM model, generated by the implantation of a rat mesothelioma cell line, IL45-*luc,* underneath parietal pleura of immunocompetent rats (19). IL45-*luc* cells cultured *in vitro* in the presence of 10% FBS expressed high levels of *Gli1*, *Ptch1* and *Smo*, however mRNA levels of all Hh ligands were very low- or undetectable. Interestingly, a robust increase of *Dhh* mRNA level was detected in *in vivo* tumor compared to *in vitro* cell culture (figure 2a). Expression levels of other Hh pathway components, *Gli1*, *Gli2* and *Gli3* were reduced in tumor derived from IL45-*luc* compared to *in vitro. Hhip*, Hh pathway target gene and its' negative regulator, became detectable only *in vivo* (figure 2a). Primary cells isolated from IL45-*luc* derived tumors, cultured in 3%O_2 without serum continued to express *Dhh* but expressed only low levels of *Gli1* when compared with *in vivo* or IL45-*luc* cultured in the presence of 10% FBS (figure 2a).

Histological assessment of the orthotopic tumors revealed that tumor cells were surrounded by stroma including extracellular matrix (ECM)/lymphocytes/fibroblasts/blood vessels (figure 1b). Similar to human MPM, immunohistochemical analysis revealed predominant cytoplasmic localization of DHH in tumor cells but not in the stroma (S) whereas GLI1 was expressed in both tumor (T) and stroma fractions (figure 1b).

The treatment with vismodegib did not downregulate Hh target genes in rat mesothelioma cell lines *in vitro*

In terms of the sensitivity of these cell lines to Hh pathway inhibition *in vitro*, IL45 and IL45-*luc* responded to vismodegib at the same extent after 72 hours treatment (figure 2b). Growth inhibitory

Author Manuscript Published OnlineFirst on February 2, 2016; DOI: 10.1158/1535-7163.MCT-15-0583
Author manuscripts have been peer reviewed and accepted for publication but have not yet been edited.

effect was observed when using > 20 μM of vismodegib in both cell lines. This is in line with the literature reporting the effective concentration of vismodegib *in vitro* (7, 27). However, this concentration is much higher than the effective concentration reported for Hh responsive cell lines (13, 27). Vismodegib could not suppress the expression of Hh target genes, *Gli1and Ptch1* (figure 2c). We therefore employed colony formation assay to assess long term treatment effects (10 days). Although, a lower amount of vismodegib was required to inhibit colony formation of IL45 and IL45-*luc* cells (figure 2b) compared to short term treatment, this effective concentration was still higher than that required for Hh pathway inhibition (27). The unresponsiveness of IL45 and IL45-*luc* to vismodegib in terms of Hh target genes downregulation *in vitro* implied the lack of constitutive activation of Hh pathway in these cell lines.

Treatment with vismodegib *in vivo* suppresses Hh signaling pathway mainly in stroma and induced significant reduction of tumor size and caused tumor growth delay

Thus, we investigated the effects of the SMO antagonist, vismodegib, in the rat MPM model to further elaborate the role of Hh signaling. The experimental scheme is depicted in figure 3a. SMO antagonist, vismodegib was administered with the effective dosage applied in preclinical studies (22). Six days later, we observed that tumor volume measured by MRI was significantly reduced in the treated group compared to control (3 folds difference, p=0.03) (figure 3b). Consistently, significant reduction of macroscopic tumor volume (p=0.03) of the treated group was detected (figure 3d). Tumor growth monitored by Bli seems to be reduced in the treated group compared to control (see images in figure 3e). Nevertheless the overall growth suppression was not statistically significant comparing control with treatment group, which may be in part due to the high standard deviation of the measurement (figure 3e).

Robust reduction of mRNA levels of *Gli1 Hhip* and *Ptch1* was observed *in vivo* after vismodegib treatment compared to control group (figure 4a). No significant change in the expression of *Dhh*, *Gli2* and *Gli3* was detected (figure 4a). The analysis in skin samples also showed strong down regulation of *Gli1* (figure 4a), confirming the efficacy of vismodegib in the inhibition of the Hh pathway in this rat model. We further analyzed GLI1, PTCH1, HHIP and DHH expression by immunohistochemistry. Tumor fraction was clearly distinguishable based on large cell size, big nuclei, less spindeloid shape than fibroblast (figure 1b). Slightly reduced GLI1 expression in tumor cells was observed (figure 4b, 4c). Interestingly, we observed significant down regulation of GLI1 and HHIP in the stromal fraction of treated rats compared to controls (figure 4b, 4c). We did not detect any change

Author Manuscript Published OnlineFirst on February 2, 2016; DOI: 10.1158/1535-7163.MCT-15-0583
Author manuscripts have been peer reviewed and accepted for publication but have not yet been edited.

in PTCH1 expression on the protein level, may be because change in mRNA expression levels was small compared to GLI1 or HHIP (figure 4a). DHH expression levels remained unchanged in the treated rats (figure 4b).

Vismodegib treatment reduces tumor cell proliferation rate but does not induce cell death

Immunohistochemical analysis of Ki-67 and p-H3 (phospho-histone H3) indices was performed to assess proliferation and mitosis of tumor cells, respectively (figure 4d). Significant reduction of both Ki-67 and p-H3 index in the treated group versus control was detected. TUNEL staining showed a very low percentage of dead cells without central necrosis in both control and treated tumors. No significant difference of TUNEL positivity was observed in the treated group compared to controls (figure 4d).

Primary cells isolated from *in vivo* rat tumor model, cultured in 3%O_2 without serum sustain the expression of *Dhh* but are not sensitive to vismodegib

We previously observed that primary human MPM cells cultured in the physiological condition (in own conditioned medium with growth factors (see method) and 3%O_2) could sustain stemness and DHH secretion (5). Therefore we isolated primary cells from the orthotopic rat tumors and cultured them in this condition. We indeed detected increased *Dhh* expression in primary cells cultured in 3%O_2 without serum compared to IL45-*luc* cultured in 10% serum and 20% O_2 (figure 2a). This finding is consistent in primary cells isolated from 3 different animals (supplementary figure s1). We could not observe any correlation between *Gli1* and *Dhh* expression in these cells (supplementary figure s1). The response of primary cells to vismodegib is identical to what we observed in IL45-*luc* cultured in serum (figure 5a). No difference in response to vismodegib was detected in cells isolated from control and vismodegib treated rats (figure 5a). No down regulation of *Gli1* or *Ptch1* was observed under this culture condition in response to SAG or vismodegib treatment (figure 5b, supplementary figure s2). The response of tumor cells to vismodegib (determined by IC50) did not correlate with the expression levels of Hh pathway components (*Dhh*, *Smo*, *Ptch1*, *Gli1*) (figure 5c).

Treatment with vismodegib causes downregulation of *Fibronectin*, *Vegf*, and *Lif* expression, the previously described indirect Hh pathway targets in fibroblast

We could not observe downregulation of other canonical Hh target genes namely *CyclinD1* and *Abcg2* (figure 6a) (28, 29). Since in our model we observed that vismodegib treatment induced stronger GLI1 down regulation in the stromal compared to the tumor compartment, we hypothesized that Hh pathway activation occurred primarily in a paracrine fashion. We therefore focused on the effects of vismodegib in stroma in order to understand the mechanisms leading to the reduced proliferation hence tumor

Author Manuscript Published OnlineFirst on February 2, 2016; DOI: 10.1158/1535-7163.MCT-15-0583
Author manuscripts have been peer reviewed and accepted for publication but have not yet been edited.

growth delay. Previous experiments suggest that antagonization of Hh pathway in fibroblasts reduces the production of extracellular matrix (ECM), cytokines and growth factors (13-15). Therefore we analyzed mRNA levels of the ECM molecules *Fibronectin* (*Fn1*) and *Collagen* (*Col1a2*). We did not detect differences in *Collagen* mRNA levels, may be due to the fact that the expression of collagen is too abundant (*Col1a2* Ct~18 versus loading control Histone H3 Ct~22) to allow us to observe any difference. Nevertheless, we could detect a downregulation of *Fn1* mRNA levels in the treated group (figure 6a). We further analyzed Fibronectin expression by immunohistochemistry and observed significantly reduced levels of Fibronectin in the treated group compared to controls (supplementary figure s3). Thus, one possibility is that the difference in tumor volume between control and vismodegib treated tumor might be in part due to reduced ECM content. In addition, Shh was shown to stimulate the secretion of VEGF and LIF (14) from fibroblasts. Indeed, in agreement with this finding, we observed here *in vivo*, a significant reduction on *Vegf* and *Lif* mRNA in the treated group compared to control (figure 6a).

Culture supernatant of primary cells from *in vivo* rat tumors stimulated *Gli1*, *Ptch1* and *Fn1* expression of NIH3T3 cells

To confirm paracrine activation of Hh signaling between tumor cells and stroma, we employed *in vitro* assay using mouse embryonic fibroblast cells (NIH3T3). NIH3T3 were treated with the supernatant collected from primary cells derived from a rat tumor. 72 hours after the incubation with rat MPM supernatant in 3%O_2, we observed a strong upregulation of *Gli1* and *Ptch1* in NIH3T3 cells which was reduced by the treatment with vismodegib. The treatment with 50 nM SAG induced slightly *Gli1* upregulation but not *Ptch1* (figure 6b). This may be explained by the fact that *Ptch1* expression is not strongly induced by the Hh pathway activation compared to *Gli1* (eg. culture supernatant of primary cells induced 4 times *Gli1* upregulation but only 1.8 *Ptch1* upregulation (figure 6b)). NIH3T3 treated with SAG and rat supernatant showed upregulation of *Fn1* which was suppressed by vismodegib treatment. Similar to the effect seen with the rat MPM cell culture supernatant, NIH3T3 treated with primary human MPM cell culture supernatant showed upregulation of *Gli1*, *Ptch1* and *Fn1* (supplementary figure s4).

Discussion

In this study we provide new evidence regarding the importance of Hh signaling in MPM stroma in the maintenance of MPM tumor growth. The Hh pathway was activated in both tumor and

Author Manuscript Published OnlineFirst on February 2, 2016; DOI: 10.1158/1535-7163.MCT-15-0583
Author manuscripts have been peer reviewed and accepted for publication but have not yet been edited.

stroma of MPM human tissues and the orthotopic immunocompetent rat model. After continuous treatment with the SMO antagonist, vismodegib, *in vivo,* pronounced and significant down regulation of the well-known Hh target genes, GLI1 and HHIP was observed only in the stromal fraction. The tumor fraction was less responsive to vismodegib *in vivo*. This is further demonstrated *in vitro* where we could not see the effect of vismodegib in the down regulation of *Gli1* in primary cells isolated from the rat MPM model. The outcomes of daily treatment with vismodegib targeting Hh pathway in the stroma included reduced tumor volume and suppressed tumor growth without inducing cell death. The treatment with vismodegib repressed indirect Hh responsive genes previously reported in fibroblasts i.e. *Fn1*, *Vegf* and *Lif*. Reduced levels of these factors may thus be responsible for tumor growth delay observed in this study

We detected the expression of Hh pathway components GLI1, HHIP and PTCH1 in human MPM specimens in both tumor and stromal fractions. Hh ligand, DHH was weakly expressed and was predominantly localized in the tumor fraction. Similar to our finding, previous studies also showed that another Hh ligand detected in human MPM, SHH, is also weakly expressed in only 47% of patients (7). The similar pattern of GLI1, PTCH1, HHIP and DHH expression was observed in orthotopic immunocompetent rat mesothelioma model. IL45-*luc* cells that were implanted orthotopically in syngeneic rats started to express *Dhh* but not the other Hh ligands. Nevertheless, *Gli1*, *Gli2* and *Gli3* expression levels were reduced *in vivo.* One most possible explanation is the presence of 10% fetal bovine serum (FBS) in *in vitro* culture medium. We observed that when the FBS was withdrawn from IL45-luc, *Gli1* expression was strongly reduced (unpublished observations). The upregulation of *Gli1* in the presence of FBS is presumably mediated by Hh independent mechanism as its expression could not be suppressed by the treatment with vismodegib. The expression of *Dhh* was still maintained when isolated and cultured without serum in 3%O_2. This observation was also documented in primary culture of human MPM cells cultured in 3%O_2 without serum in which *DHH* was the only ligand expressed (5). So far there is no obvious explanation and it remains to be elucidated why the primary culture and this *in vivo* MPM models upregulate only the expression of DHH but not other ligands.

Target genes responding to Hh pathway stimulation have been shown to be dependent on cell type and context. Shh has been shown to indirectly induce angiogenesis in juvenile and adult mice by up-regulating angiogenic factors including Vegf (30). In this study it was also demonstrated *in vitro* that only fibroblasts could secrete VEGF upon Hh pathway stimulation. Another finding showed *in vitro* that lung fibroblasts upregulated *LIF* and *VEGF* expression when treated with cell culture supernatant of

Author Manuscript Published OnlineFirst on February 2, 2016; DOI: 10.1158/1535-7163.MCT-15-0583
Author manuscripts have been peer reviewed and accepted for publication but have not yet been edited.

lung cancer cell lines that secrete SHH (14). In line with these studies, we also observed here, *in vivo,* down regulation of *Lif* and *Vegf* expression following Hh pathway suppression by vismodegib. In addition, cell culture supernatant of primary rat and human MPM cells could stimulate *Gli1*, *Ptch1* and *Fn1* expression in NIH3T3 when incubated at 3%O_2, 37ºC for but not at atmospheric O_2 level. Under this culture condition, we did not detect an increase in *Lif* and *Vegf* expression in NIH3T3 cells treated either with cell culture supernatant or SAG (unpublished observations). One possible reason is that the tested *in vitro* condition does not fully recapitulate *in vivo* tumor micro-environment. Although *Fn1*, *Lif* and *Vegf* can also be produced by some MPM cells, (31-33), it is not known whether these are Hh responsive genes in tumor. Based on our results being i) stroma was the main part affected by vismodegib ii) *Fn1, Lif* and *Vegf* have been so far described to be regulated by the Hh pathway only in fibroblast, we presume that the effects of vismodegib that we observed herein results primarily from the modulation of fibroblasts. Interestingly, *Vegf* promoters do not contain GLI1 binding consensus sequence (14). Thus, the effect of vismodegib on *Vegf* expression could mostly stem from indirect regulation. One mediator could be hypoxia as a study in pancreatic cancer demonstrated that SHH secreted from tumors stabilized HIF1α, a known transcription factor of VEGF, in pancreatic fibroblasts (34).

In vitro, high concentration of vismodegib (>20 μM) was required to suppress the growth of IL45 and IL45-*luc* cells. This concentration is in the range reported for most human cancer cell lines having ligand dependent activation as well as human MPM cells (IC50 = 15-20 μM) (7, 27). Nevertheless, the concentration used in these studies was far higher than the effective concentration (100-500 nM) of vismodegib required to completely inhibit Hh pathway activity of responsive cell lines (13, 27). In the contrast to these studies, we could not observe a significant reduction of *Gli1* expression after exposing IL45 cells to various concentrations of vismodegib. Similarly, a study in various other cancer cell lines showed that the treatment with Hh antagonist as well as ligand blocking antibody did not induce down regulation of *GLI1*, the well-described Hh target gene *in vitro* (13). Thus, it is still a matter of debate whether the growth inhibitory effect of SMO antagonist observed *in vitro* is only due to off-target effects when applied at high concentration. Vismodegib was shown to inhibit ABCG2 drug transporter (35) as well as cellular calcium homeostasis (36) when applied at a high concentration. Thus, the lack of *Gli1* downregulation after treatment with vismodegib *in vitro* suggested that the growth inhibitory effect observed herein may result from off target effects. Nonetheless, given the heterogeneic nature of MPM, the effect may depend on the cell lines employed. Indeed, Shi et al

(5) described that only 4 out of 6 cell lines cultured in 3%O_2 without serum showed down-regulation of *Gli1* in response to SMO antagonist treatment.

GLI1 has been shown to be activated in Hh independent fashion, *via* cross-talking with other oncogenic pathways such as KRAS, EGFR and mTOR (8, 37). A recent study demonstrated that GLI1 was highly expressed in some MPM tumors of which SHH expression was absent (7), suggesting a possible role of GLI1 activation in Hh signaling independent manner (13). A recent study suggests a better proliferation inhibitory effect of GLI1 inhibitor (GANT61) compared to vismodegib on MPM cells (7). Nevertheless, the role of non-canonical ligand dependent Hh activation in MPM has to be explored in more detail. Besides, agents targeting GLI1 have not yet been available for clinical use.

We have the advantage of using an immunocompetent pre-clinical model that contains clinically relevant stromal components including extracellular matrix, fibroblasts and immune cells. However, there are limitations of our study including short treatment and observation period; the major reason for this limitation being the aggressiveness of the model that influences animal well-being. Vismodegib was shown to inhibit the drug transporter, ABCG2 with the IC50 of more than 1 μM (35). ABCG2 was important for the efflux of Bli substrate luciferin, thus the treatment with vismodegib caused false positive Bli signal (38). We indeed observed the effect of vismodegib in interfering luciferin efflux in IL45-*luc* at concentration of > 1 *μM in vitro*, (sustained Bli decline rate, supplementary figure s5). A large proportion of circulating vismodegib (98% in rats (39)) is bound to serum alpha 1-acid glycoprotein (AAG). An *in vivo* study in mice receiving 100 mg/kg demonstrated a C_{max} of 35 μM for total vismodegib (22). Thus we estimate to have approximately 0.7 μM of unbound vismodegib in the rat serum. This concentration still does not interfere with Bli. Moreover, persisting Bli signal should be observed when ABCG2 was inhibited (38), but Bli kinetics after the substrate administration in control and treated animals are similar (supplementary figure s5). These data ruled out the possible interference of vismodegib on the detection of tumor by Bli in this study.

Here, we employed an immunocompetent preclinical model of MPM to demonstrate that the Hh pathway inhibition in MPM affects the production of extracellular matrix and cytokines, factors crucial for tumor progression. Our study also provides novel information regarding the role of Hh signaling in MPM in stroma.

Acknowledgments

The present study was supported by the Swiss National Science Foundation grants to Isabelle Opitz. We thank Prof. Martin Pruschy for providing the IVIS machine; Dr. Vet. Med. Margarete Arras, Dr. Vet. Med. Nikola Cesarovic and Dr. Vet. Med. Thea Fleischman for their kind assistance in designing the anaesthetic and analgesic protocols. In addition, we thank Dr. Michaela Kirschner for thoroughly reading and providing insightful comments for the manuscript.

References

1. Carbone M, Kratzke RA, Testa JR. The pathogenesis of mesothelioma. Semin Oncol. 2002;29:2-17.
2. Peto J, Decarli A, La Vecchia C, Levi F, Negri E. The European mesothelioma epidemic. Br J Cancer. 1999;79:666-72.
3. Lanphear BP, Buncher CR. Latent period for malignant mesothelioma of occupational origin. Journal of occupational medicine : official publication of the Industrial Medical Association. 1992;34:718-21.
4. Weder W, Stahel RA, Bernhard J, Bodis S, Vogt P, Ballabeni P, et al. Multicenter trial of neo-adjuvant chemotherapy followed by extrapleural pneumonectomy in malignant pleural mesothelioma. Ann Oncol. 2007;18:1196-202.
5. Shi Y, Moura U, Opitz I, Soltermann A, Rehrauer H, Thies S, et al. Role of hedgehog signaling in malignant pleural mesothelioma. Clin Cancer Res. 2012;18:4646-56.
6. Zhang Y, He J, Zhang F, Li H, Yue D, Wang C, et al. SMO expression level correlates with overall survival in patients with malignant pleural mesothelioma. J Exp Clin Cancer Res. 2013;32:7.
7. Li H, Lui N, Cheng T, Tseng HH, Yue D, Giroux-Leprieur E, et al. Gli as a novel therapeutic target in malignant pleural mesothelioma. PLoS One. 2013;8:e57346.
8. Mimeault M, Batra SK. Frequent deregulations in the hedgehog signaling network and cross-talks with the epidermal growth factor receptor pathway involved in cancer progression and targeted therapies. Pharmacological reviews. 2010;62:497-524.
9. Reifenberger J, Wolter M, Knobbe CB, Kohler B, Schonicke A, Scharwachter C, et al. Somatic mutations in the PTCH, SMOH, SUFUH and TP53 genes in sporadic basal cell carcinomas. The British journal of dermatology. 2005;152:43-51.
10. Schwalbe EC, Lindsey JC, Straughton D, Hogg TL, Cole M, Megahed H, et al. Rapid diagnosis of medulloblastoma molecular subgroups. Clin Cancer Res. 2011;17:1883-94.
11. Gupta S, Takebe N, Lorusso P. Targeting the Hedgehog pathway in cancer. Therapeutic advances in medical oncology. 2010;2:237-50.
12. Karlou M, Lu JF, Wu G, Maity S, Tzelepi V, Navone NM, et al. Hedgehog signaling inhibition by the small molecule smoothened inhibitor GDC-0449 in the bone forming prostate cancer xenograft MDA PCa 118b. Prostate. 2012;72:1638-47.
13. Yauch RL, Gould SE, Scales SJ, Tang T, Tian H, Ahn CP, et al. A paracrine requirement for hedgehog signalling in cancer. Nature. 2008;455:406-10.
14. Bermudez O, Hennen E, Koch I, Lindner M, Eickelberg O. Gli1 mediates lung cancer cell proliferation and Sonic Hedgehog-dependent mesenchymal cell activation. PLoS One. 2013;8:e63226.
15. Spivak-Kroizman TR, Hostetter G, Posner R, Aziz M, Hu C, Demeure MJ, et al. Hypoxia triggers hedgehog-mediated tumor-stromal interactions in pancreatic cancer. Cancer Res. 2013;73:3235-47.
16. Felley-Bosco E, Opitz I, Meerang M. Hedgehog signaling in malignant pleural mesothelioma. Genes. 2015;manuscript accepted.
17. Lim CB, Prele CM, Cheah HM, Cheng YY, Klebe S, Reid G, et al. Mutational analysis of hedgehog signaling pathway genes in human malignant mesothelioma. PLoS One. 2013;8:e66685.
18. Craighead JE, Akley NJ, Gould LB, Libbus BL. Characteristics of tumors and tumor cells cultured from experimental asbestos-induced mesotheliomas in rats. Am J Pathol. 1987;129:448-62.
19. Shi Y, Hollenstein A, Felley-Bosco E, Fraefel C, Ackermann M, Soltermann A, et al. Bioluminescence imaging for in vivo monitoring of local recurrence mesothelioma model. Lung Cancer. 2011;71:370-1.
20. Friedrich J, Seidel C, Ebner R, Kunz-Schughart LA. Spheroid-based drug screen: considerations and practical approach. Nat Protoc. 2009;4:309-24.
21. Lardinois D, Jung FJ, Opitz I, Rentsch K, Latkoczy C, Vuong V, et al. Intrapleural topical application of cisplatin with the surgical carrier Vivostat increases the local drug concentration in an immune-competent rat model with malignant pleuromesothelioma. J Thorac Cardiovasc Surg. 2006;131:697-703.
22. Wong H, Alicke B, West KA, Pacheco P, La H, Januario T, et al. Pharmacokinetic-pharmacodynamic analysis of vismodegib in preclinical models of mutational and ligand-dependent Hedgehog pathway activation. Clin Cancer Res. 2011;17:4682-92.
23. Meerang M, Boss A, Kenkel D, A. B-T, Berard K, Lauk O, et al. Evaluation of Imaging Techniques for the Assessment of Tumor Progression in an Orthotopic Rat Model of Malignant Pleural Mesothelioma. Eur J Cardio-Thorac. 2014;In press.
24. Frei C, Opitz I, Soltermann A, Fischer B, Moura U, Rehrauer H, et al. Pleural mesothelioma side populations have a precursor phenotype. Carcinogenesis. 2011;32:1324-32.

25. Makela JA, Saario V, Bourguiba-Hachemi S, Nurmio M, Jahnukainen K, Parvinen M, et al. Hedgehog signalling promotes germ cell survival in the rat testis. Reproduction. 2011;142:711-21.
26. Knobel PA, Kotov IN, Felley-Bosco E, Stahel RA, Marti TM. Inhibition of REV3 expression induces persistent DNA damage and growth arrest in cancer cells. Neoplasia. 2011;13:961-70.
27. You M, Varona-Santos J, Singh S, Robbins DJ, Savaraj N, Nguyen DM. Targeting of the Hedgehog signal transduction pathway suppresses survival of malignant pleural mesothelioma cells in vitro. J Thorac Cardiovasc Surg. 2014;147:508-16.
28. Kenney AM, Rowitch DH. Sonic hedgehog promotes G(1) cyclin expression and sustained cell cycle progression in mammalian neuronal precursors. Mol Cell Biol. 2000;20:9055-67.
29. Duman-Scheel M, Weng L, Xin S, Du W. Hedgehog regulates cell growth and proliferation by inducing Cyclin D and Cyclin E. Nature. 2002;417:299-304.
30. Pola R, Ling LE, Silver M, Corbley MJ, Kearney M, Blake Pepinsky R, et al. The morphogen Sonic hedgehog is an indirect angiogenic agent upregulating two families of angiogenic growth factors. Nat Med. 2001;7:706-11.
31. Pass HI, Stevens EJ, Oie H, Tsokos MG, Abati AD, Fetsch PA, et al. Characteristics of Nine Newly Derived Mesothelioma Cell Lines. The Annals of Thoracic Surgery. 1995;59:835-44.
32. Ferriola PC, Stewart W. Fibronectin expression and organization in mesothelial and mesothelioma cells. The American journal of physiology. 1996;271:L804-12.
33. Li Q, Yano S, Ogino H, Wang W, Uehara H, Nishioka Y, et al. The therapeutic efficacy of anti vascular endothelial growth factor antibody, bevacizumab, and pemetrexed against orthotopically implanted human pleural mesothelioma cells in severe combined immunodeficient mice. Clin Cancer Res. 2007;13:5918-25.
34. Bailey JM, Mohr AM, Hollingsworth MA. Sonic hedgehog paracrine signaling regulates metastasis and lymphangiogenesis in pancreatic cancer. Oncogene. 2009;28:3513-25.
35. Zhang Y, Laterra J, Pomper MG. Hedgehog pathway inhibitor HhAntag691 is a potent inhibitor of ABCG2/BCRP and ABCB1/Pgp. Neoplasia. 2009;11:96-101.
36. Tian F, Schrodl K, Kiefl R, Huber RM, Bergner A. The hedgehog pathway inhibitor GDC-0449 alters intracellular Ca2+ homeostasis and inhibits cell growth in cisplatin-resistant lung cancer cells. Anticancer Res. 2012;32:89-94.
37. Wang Y, Ding Q, Yen CJ, Xia W, Izzo JG, Lang JY, et al. The crosstalk of mTOR/S6K1 and Hedgehog pathways. Cancer Cell. 2012;21:374-87.
38. Zhang Y, Bressler JP, Neal J, Lal B, Bhang HE, Laterra J, et al. ABCG2/BCRP expression modulates D-Luciferin based bioluminescence imaging. Cancer Res. 2007;67:9389-97.
39. Wong H, Chen JZ, Chou B, Halladay JS, Kenny JR, La H, et al. Preclinical assessment of the absorption, distribution, metabolism and excretion of GDC-0449 (2-chloro-N-(4-chloro-3-(pyridin-2-yl)phenyl)-4-(methylsulfonyl)benzamide), an orally bioavailable systemic Hedgehog signalling pathway inhibitor. Xenobiotica; the fate of foreign compounds in biological systems. 2009;39:850-61.

Author Manuscript Published OnlineFirst on February 2, 2016; DOI: 10.1158/1535-7163.MCT-15-0583
Author manuscripts have been peer reviewed and accepted for publication but have not yet been edited.

Figure legends

Figure 1. Analysis of Hh pathway activation in human MPM specimens and rat MPM model in tumor and stromal fractions. a) Immunohistochemical detection of GLI1, DHH, PTCH1 and HHIP in tumor (T) and stroma (S) and box plot of semi-quantitative expression levels (H-score) of GLI1 and DHH in146 MPM specimens, and PTCH1 and HHIP in 8 MPM specimens (lines indicate medians). **b)** Histology of rat MPM model revealed cellular areas of closely packed spindled tumor cells (T) with relatively large, irregular nuclei, adjacent to stroma (S) containing fibroblasts (organized small spindle cells, *), blood vessels (X) and inflammatory cells (small round cells with dense blue chromatin; arrow). Of note is the presence of some fibroblasts and inflammatory cells also in the tumor area. Scatter plot shows semi-quantitative expression levels of GLI1, DHH, PTCH1 and HHIP (H-score) of 6 tumors (lines indicate medians).

Figure 2. **The comparison of Hh pathway activation *in vitro* and *in vivo* rat MPM model.**

a) Expression levels (mRNA) of pathway components were monitored in IL45-*luc* cultured in 10% serum, primary cell culture in 3% O_2 without serum compared to tumor from the rat model (*in vivo*). **b)** Cell growth measurement by MTT (left) and colony formation assay (right) shows that IL45-*luc* and the parental line (IL45) cultured in 20%O_2 with serum are identically sensitive to vismodegib (Data are given in mean $\pm$ SD; *, $p<0.05$; **, $p<0.001$; ***, $p<0.0001$). **c, d)** IL45 parental cells were exposed to increasing concentration of vismodegib and measured for the down regulation of hedgehog pathway target gene (*Gli1 and Ptch1*) in addition to *Gli2* and *Gli3*. No significant suppression of all genes was observed upon the treatment course (24 and 48 hours).

Figure 3. Daily treatment with vismodegib effectively reduces tumor volume and growth in *vivo*.

a) Experimental scheme of orthotopic rat MPM model and the treatment with vismodegib. **b)** Box and whisker plot of tumor volume quantified from MRI images performed at the last day of treatment (representative images are shown in **(c)**. **d)** Macroscopic tumor volume performed at the last day of treatment. **e)** Tumor growth monitored by bioluminescence (total flux) over a period of 6 days and representative images. (Data are given in mean $\pm$ SD; *, $p<0.05$; **; $p<0.001$; ***; $p<0.0001$)

Figure 4. Efficient down regulation of Hh signaling and reduce tumor cell growth following the treatment with vismodegib. a) mRNA levels of Hh target genes, *Gli1* is strongly reduce in skin and tumor of vismodegib treated rats. Expression level of other GLI1 target genes, *Ptch1* and *Hhip* is also reduced in treated tumor compared to control. *Dhh, Gli2, Gli3* expression remains unchanged. **b)** Immunohistochemical staining of GLI1 and HHIP showing reduced expression (intensity and

frequency) in treated compared to control. More GLI1, HHIP negative stromal cells are present in the treated rat (see circles T:tumor, S:stroma). **c)** Quantitative analysis histo(H)-score of GLI1, HHIP, PTCH1 and DHH staining showing pronounced GLI1 and HHIP downregulation in stromal fractions. **d)** Proliferation (Ki-67 positive), mitotic (phospho-histone H3 positive) indices are significantly reduced in the treated group. No change in necrosis and apoptosis level (TUNEL positive nuclei) is observed between groups. (C: Control; n=6, T: Treated; n=6, Data are given in mean ± SD; *, p<0.05; **; p<0.001; ***; p<0.0001)

Figure 5. Vismodegib dose-dependently suppresses growth of mesothelioma cells but could not suppress Hh pathway *in vitro*.

a) Primary cells isolated from 4 different rat tumors cultured in 3% O_2 without serum and IL45-luc cell line cultured 20%O_2 were exposed to increasing concentration of vismodegib and measured for viability. No difference in terms of sensitivity to vismodegib was observed (Data are given in mean ± SD). **b)** Two lines of primary cell (isolated from control rats) were treated with vismodegib for 24 hours and analyzed for the down regulation of *Gli1*. No significant suppression of *Gli1* was observed. **c)** IC50 of vismodegib determined in 4 cell lines after 72 hour treatment (MTT assay) **d)** the expression levels of Hh pathway components (*Dhh, Smo, Ptch1, Gli1*) of the 4 cell lines showing no correlation with their sensitivity to vismodegib

Figure 6. Daily treatment with vismodegib causes down regulation of previously described fibroblast Hh responsive genes. a) mRNA levels of canonical Hh target gene such as *CyclinD1*, *Abcg2* remained unchanged in vismodegib treated group compared to control. Previously described fibroblast Hh responsive genes i.e. *Fibronectin*, *Vegf* and *Lif* mRNA levels were reduced in vismodegib treated group. (C: Control; n=6, T: Treated; n=6, Data are given in mean ± SD; *, p<0.05; **; p<0.001; ***; p<0.0001) **b)** Mouse embryonic fibroblast NIH3T3 cells were treated with supernatant collected from primary culture of rat MPM cells. Treatment with SMO agonist (SAG) was employed as a positive control. *Gli1*, *Ptch1* and *Fn1* expression levels were analyzed after 72 hours incubation at 37 °C 3%O_2 (data represent mean of triplicates ± SD)

Figure 1

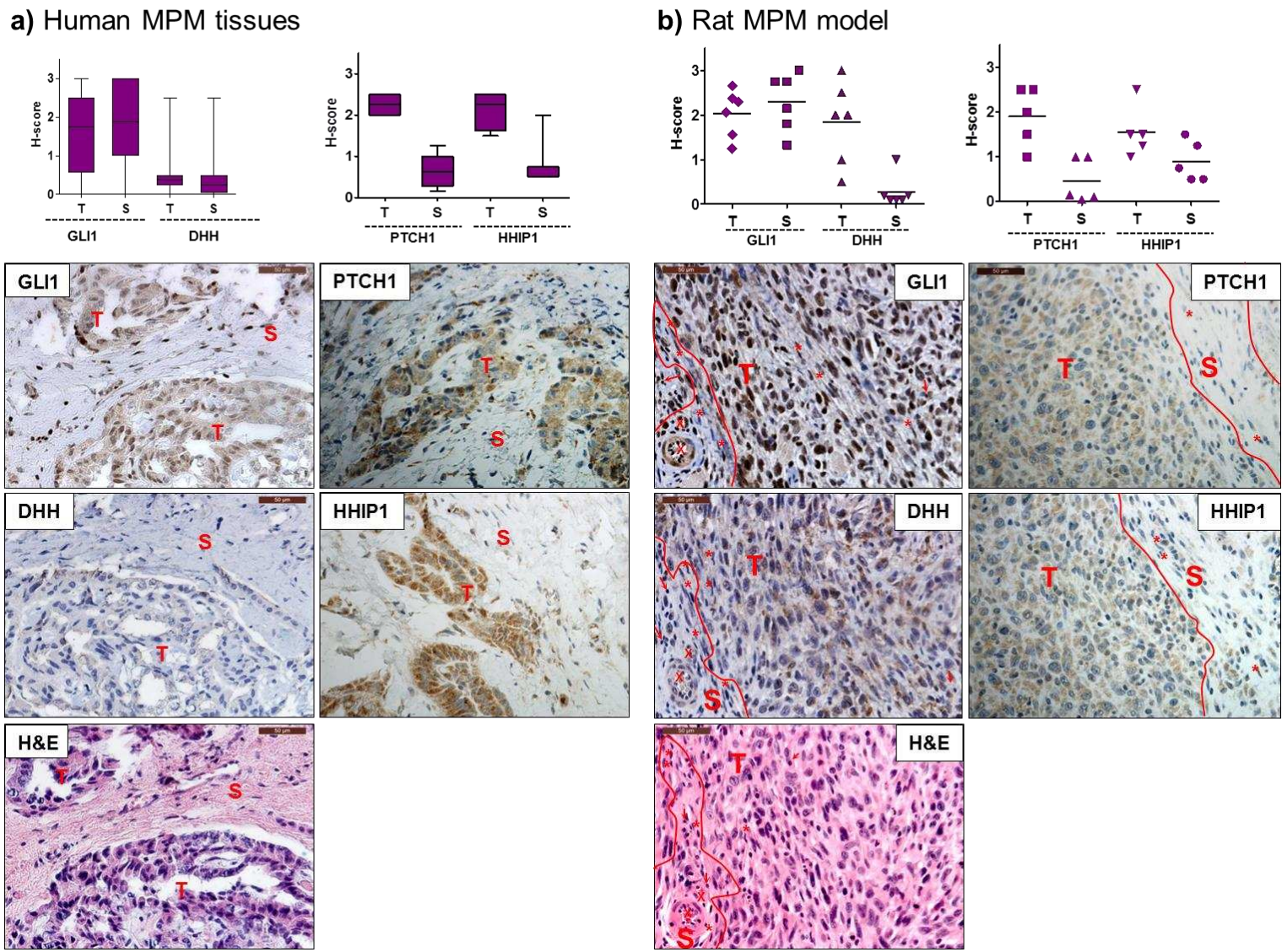

Figure 2

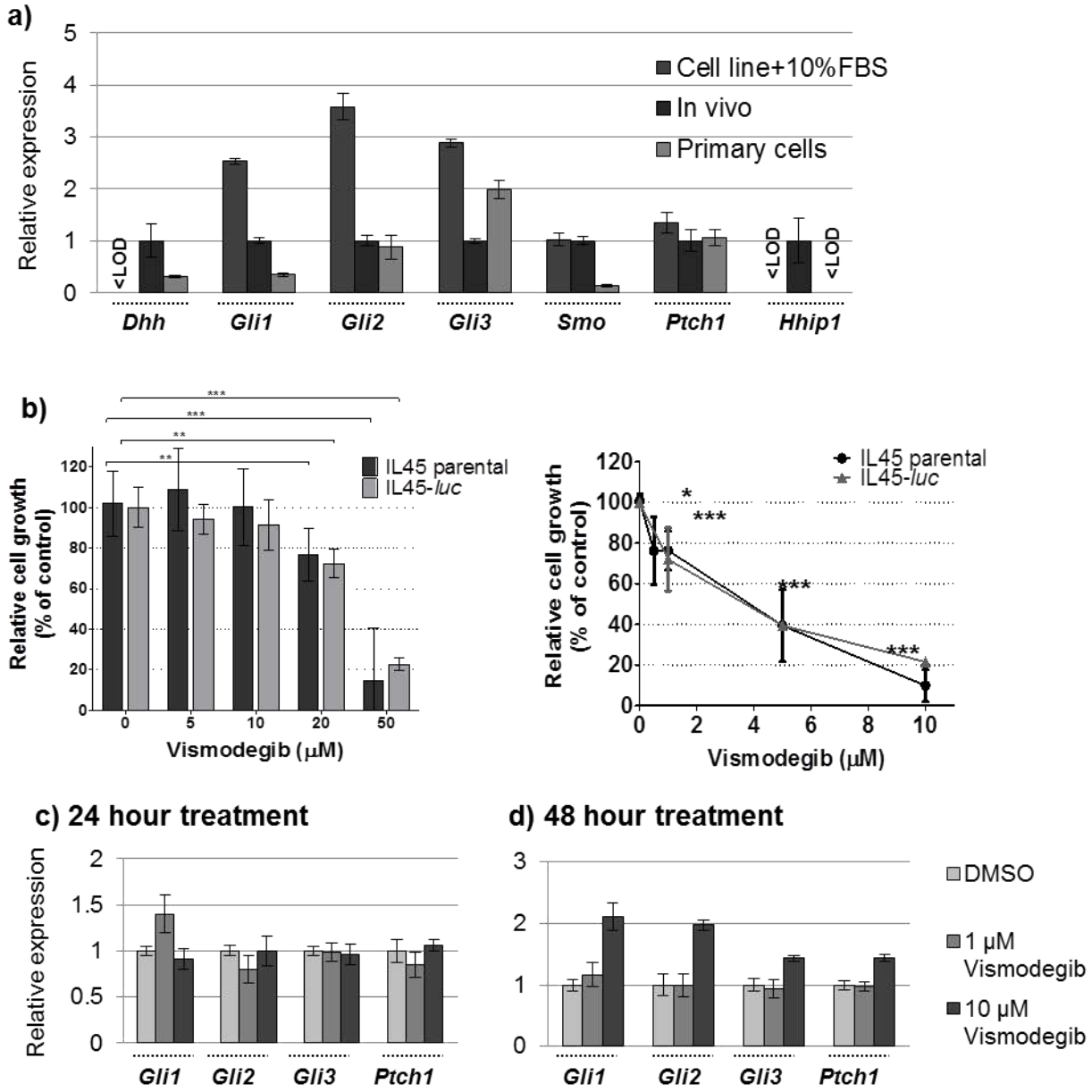

Figure 3

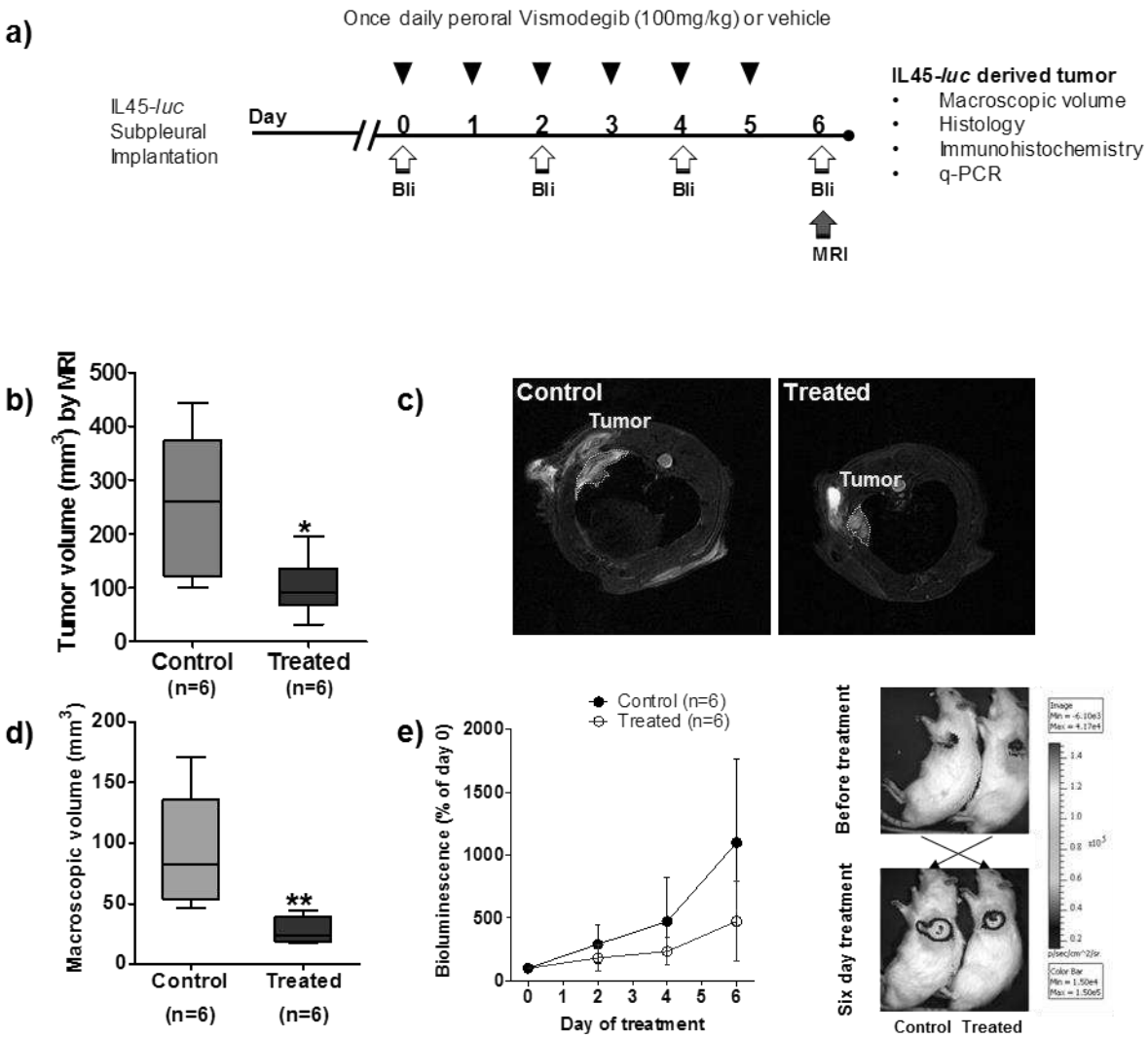

Figure 4

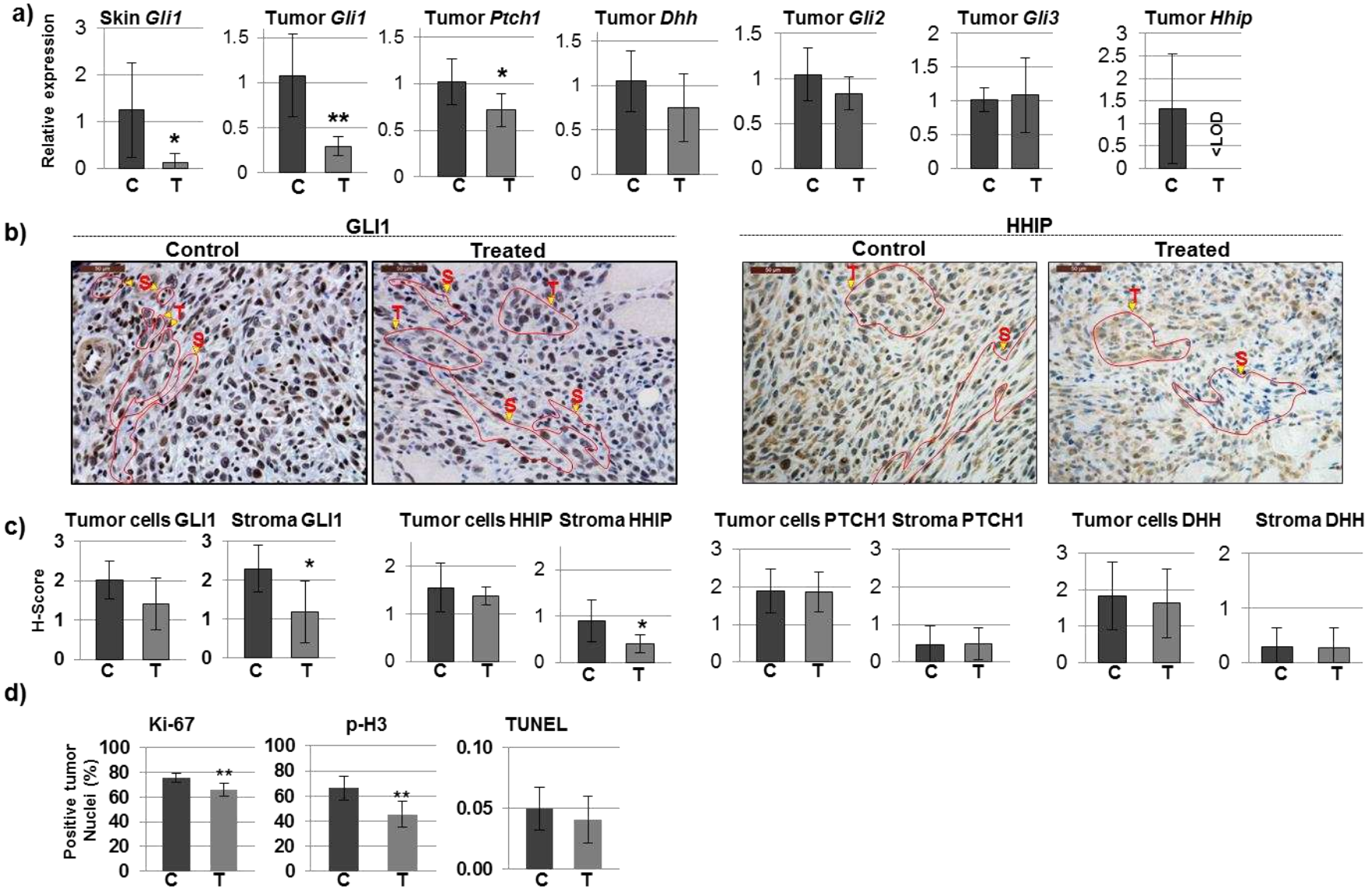

Figure 5

a)

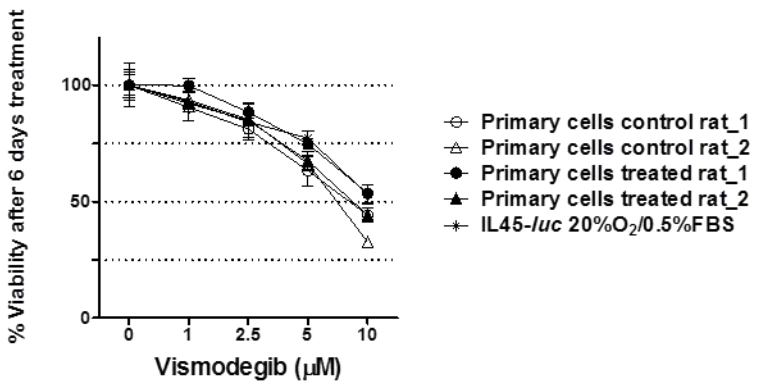

b)

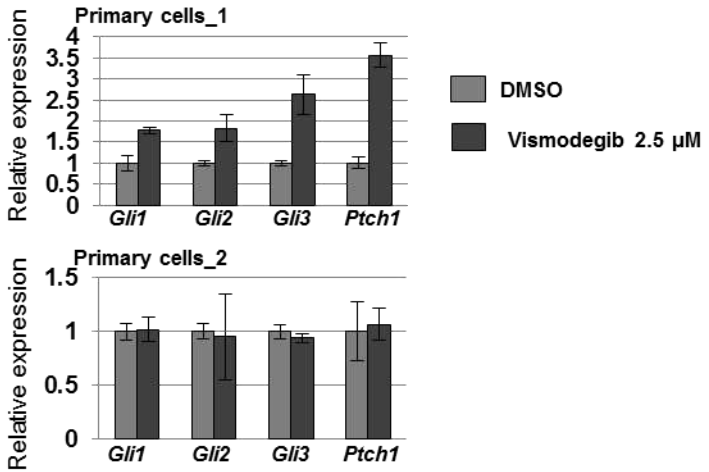

c)

IC50 Vismodegib (μM)	
1) Primary cells control rat_1	8.7
2) Primary cells control rat_2	8.1
3) Primary cells treated rat_1	13.9
4) IL45-luc 20%O_2/0.5%FBS	13.3

d)

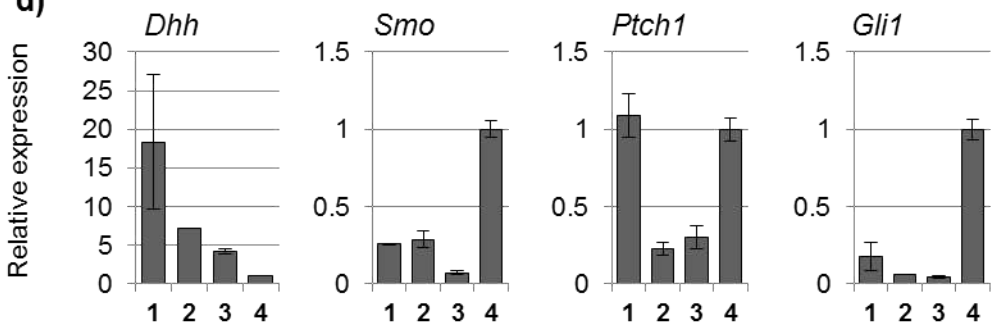

Figure 6

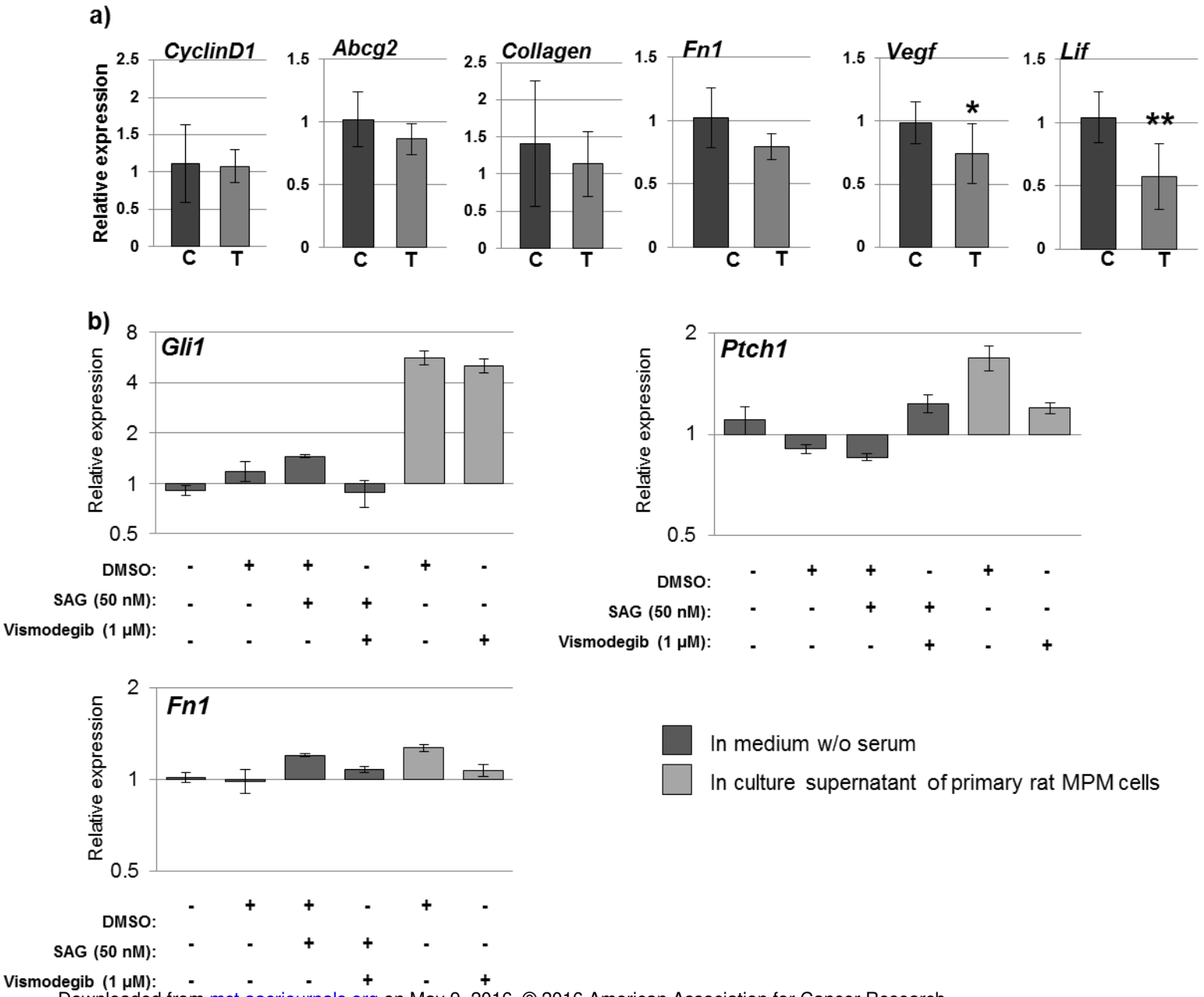

AACR American Association for Cancer Research

Molecular Cancer Therapeutics

Antagonizing the Hedgehog Pathway with Vismodegib Impairs Malignant Pleural Mesothelioma Growth In Vivo by Affecting Stroma

Mayura Meerang, Karima Bérard, Emanuela Felley-Bosco, et al.

Mol Cancer Ther Published OnlineFirst February 2, 2016.